European Congress on Computational Methods in Applied Sciences and Engineering
ECCOMAS 2000
Barcelona, 11-14 September 2000

CALCULATIONS OF 3D WAKES IN STRATIFIED FLUIDS

M.Y. Forestier, R. Pasquetti and R. Peyret

Laboratoire J.A. Dieudonné, UMR CNRS 6621
Université de Nice-Sophia Antipolis, Parc Valrose, 06108 Nice cedex 2, France

Key words: Wake flows, stratified fluids, spectral methods, multi-domain techniques, outflow boundary conditions, penalty technique.

Abstract. *A spectral method is used for the computation of wakes in 3D thermally stratified fluids with one homogeneous direction. It is based on a Chebyshev-Fourier multi-domain solver of the velocity and temperature governing equations. For the sake of stability, the part of the convective terms associated with the mean flow velocity is handled implicitly. The obstacle is modeled by using a penalty technique. Efficient soft outflow boundary conditions are used at the outlet. Numerical results are produced to study the influence of a weak thermal stratification on the development of the wake behind a sphere.*

1 INTRODUCTION

Our aim is to compute far wakes behind 3D obstacles, like a sphere, in stable thermally stratified fluids. To this end we use a spectral multi-domain solver of the momentum, continuity and energy equations within the Boussinesq approximation. The multi-domain technique is implemented in the elongated streamwise direction. The spanwise direction is assumed to be homogeneous and handled by Fourier expansions, whereas Chebyshev polynomials are used in the vertical and streamwise directions.

The main difficulties of the present problem come from:

- the huge amount of grid-points required for an accurate description of the flow in a 3D elongated geometry. This difficulty is overcome by the mean of parallel calculations, each subdomain being treated on a different processor.

- the outflow boundary conditions (OBC). Absorbing OBC, involving the temperature, the normal component of the velocity and the tangential components of the vorticity, are used at the outlet of the computational domain.

- the modelling of the obstacle. Spectral collocation methods being not adapted to handle geometries of complex shape, a penalty technique is used. Tests have been carried out to check the efficiency of this approach, by considering the wake of a cylinder.

These three different points are addressed in Sections 2 to 4. Section 5 is concerned with the far wake behind a sphere, the Reynolds number being equal to $Re = 300$. Three different values of the Richardson number have been used to point out the influence of the thermal stratification ($Ri = \{0.0, 0.04, 0.25\}$).

2 GOVERNING EQUATIONS AND NUMERICAL TECHNIQUES

The domain is of channel type : $\Omega =]0, l[\times] - h/2, h/2[\times]0, e[$, $l >> h, e$, with an obstacle inside. The dimensionless values l, h and e are defined from a characteristic length L of this obstacle, e.g. the diameter in case of a sphere. When pointing out the entrance velocity $\boldsymbol{U}$, the governing equations read:

$$\partial_t \boldsymbol{v} + ((\boldsymbol{U} + \boldsymbol{v}).\nabla)\boldsymbol{v} = -\nabla p + Ri\, T \boldsymbol{e}_y + \frac{1}{Re}\Delta \boldsymbol{v} \quad \text{in } \Omega \times (0, t_F) \tag{1}$$

$$\nabla.\boldsymbol{v} = 0 \quad \text{in } \Omega \times (0, t_F) \tag{2}$$

$$\partial_t T + (\boldsymbol{U} + \boldsymbol{v}).\nabla T = \frac{1}{Pe}\Delta T \quad \text{in } \Omega \times (0, t_F) \tag{3}$$

with t the time, $\boldsymbol{v} = (u, v, w)$ the deviation of the velocity from the mean flow velocity $\boldsymbol{U} = (U, 0, 0)$, p a pressure term and T the temperature deviation from a reference one, $\boldsymbol{e}_y$, the unit upwards vertical vector and Ri, Re and Pe, the Richardson, Reynolds and Peclet numbers, respectively.

The previous equations have to be completed with boundary and initial conditions.

Let us denote by Γ_{in}, Γ_{out} and Γ_h the inlet, outlet and horizontal parts of the boundary respectively. Then, for the boundary conditions we assume:

- at Γ_h, free-slip conditions for the velocity and adiabaticity for the temperature,

- at Γ_{in}, a constant velocity profile, so that $\boldsymbol{v} = 0$, and Dirichlet conditions for the temperature,

- at the artificial boundary Γ_{out}, "soft OBC", as detailed in Section 3.

Moreover, as described in Section 4, the obstacle is modeled by using a penalty technique, in such a way that inside this obstacle the velocity vanishes and the temperature is governed by the heat conduction equation.

The numerical method is based on spectral approximations in space and on finite difference approximations in time. The finite difference scheme is the classical BE2/AB scheme, which makes use of the backward Euler second order approximation of the time-derivatives and of a second order Adams-Bashforth extrapolation for the convective terms. Nevertheless, for the sake of stability, the part of the advection terms associated with the mean flow velocity is also treated implicitly. The problem to be solved, at each time-step, consists then of an advection-diffusion type equation for the temperature and an Oseen type problem for the velocity :

$$\mathcal{L}^{Pe} T - \sigma T = q \quad \text{in } \Omega \tag{4}$$

$$\mathcal{L}^{Re} \boldsymbol{v} - \sigma \boldsymbol{v} - \nabla p = \boldsymbol{f} \quad \text{in } \Omega \tag{5}$$

$$\nabla . \boldsymbol{v} = 0 \quad \text{in } \Omega \tag{6}$$

$$+ Boundary\, Conditions \tag{7}$$

where $\sigma = 3/2\tau$, τ being the time-step and where q and $\boldsymbol{f}$ are easily identifiable source terms. Notice that the coupling term $RiT\boldsymbol{e}_y$ is contained in $\boldsymbol{f}$. Finally, $\mathcal{L}^{\alpha}$ is the advection-diffusion operator : $\mathcal{L}^{\alpha} = \alpha^{-1}\Delta - U\partial_x$.

Such a set of equations is linear and thus, as a result of using Fourier expansions in the z-direction, splits in a set of 2D problems associated to each Fourier mode number k, $0 \leq k \leq K$. These problems are solved by using a Chebyshev collocation method, using for all the variables the same vector space $\mathbb{P}_{I,J}$, of the polynomials of maximum degree I in x and J in y.

A multi-domain technique is implemented in the direction of great length, i.e. $\bar{\Omega} = \cup \bar{\Omega}^n$, $1 \leq n \leq N$, so that at each time-step and for each Fourier mode number k, one has to solve:

For $n = 1, ..., N$, find $\hat{\boldsymbol{v}}_k$ in $\mathbb{P}^3_{I,J}(\bar{\Omega}^n)$, $\hat{p}_k$ and $\hat{T}_k$ in $\mathbb{P}_{I,J}(\bar{\Omega}^n)$ which solve :

$$\mathcal{L}^{Pe}_k \hat{T}_k - \sigma \hat{T}_k = \hat{q}_k \quad in \quad \Omega^n_{I,J} \tag{8}$$

$$\mathcal{L}^{Re}_k \hat{\boldsymbol{v}}_k - \sigma \hat{\boldsymbol{v}}_k - \nabla_k \hat{p}_k = \hat{\boldsymbol{f}}_k(\hat{T}_k) \quad in \quad \Omega^n_{I,J} \tag{9}$$

$$\nabla_k . \hat{\boldsymbol{v}}_k = 0 \quad in \quad \bar{\Omega}^n_{I,J} \tag{10}$$

$$+ \; Boundary\, Conditions, \tag{11}$$

with the following continuity conditions: for $n = 1, ..., N-1$

$$[\![\hat{\boldsymbol{v}}_k]\!]_n = 0, [\![\hat{T}_k]\!]_n = 0, \quad (12)$$

$$[\![\hat{p}_k]\!]_n = 0, [\![\partial_x \hat{v}_k]\!]_n = 0, [\![\partial_x \hat{w}_k]\!]_n = 0, [\![\partial_x \hat{T}_k]\!]_n = 0 \quad (13)$$

In these expressions, $\bar{\Omega}^n_{I,J}$ is the set of the grid-points of sub-domain $\bar{\Omega}^n$ and $\Omega^n_{I,J}$ the sub-set of the inner points, $[\![\cdot]\!]_n$ is the jump at the interface $I_n = \bar{\Omega}^n \cap \bar{\Omega}^{n+1}$, $\mathcal{L}^\alpha_k = \alpha^{-1}(\partial_{xx} + \partial_{yy} - k^2) - U\partial_x$ and $\nabla_k = (\partial_x, \partial_y, \mathrm{i}\, k)$.

The problem (8)-(11) is first solved with homogeneous values of the unknowns at the interfaces, but taking into account the source terms and the boundary conditions. Then, the correct interface values are determined by using influence matrices to impose the continuity conditions. These influence matrices, which are computed in preliminary calculations, associate for the corresponding homogeneous problem the interface values to the jumps. Then, the full problem is solved with the correct values of T and $\boldsymbol{v}$ at the interfaces. In each sub-domain, the Oseen problem is solved in a direct way, using a Poisson equation for the pressure. The pressure at the boundary is calculated by using again an influence matrix technique, yielding a divergence-free velocity field. Nevertheless, due to the use of the same polynomial space for the pressure and velocity components ("$\mathbb{P}_N - \mathbb{P}_N$ approximation"), for the Fourier mode $k = 0$ the pressure is not unique and affected by the so-called spurious modes of pressure. Consequently, the continuity conditions $[\![\hat{p}_0]\!]_n = 0$ cannot be enforced strongly. We impose them weakly, using as trial functions a set of polynomials orthogonal to the pressure space kernel. The algorithm is described in [13] and complementary comments on the solution technique for wake type flows, i.e. when the operator $\mathcal{L}^\alpha$ is substituted to the Laplacian, are given in [4].

3 OUTFLOW BOUNDARY CONDITIONS

The problem of the OBC is difficult (see e.g. the review [6]), especially when high order methods are involved. The OBC used in our calculations are those proposed in [4], where the 2D situation was considered. Here we extend the approach to the case of 3D flows.

In [4] it is pointed out that for 2D wake type flows, when the Reynolds number is high the following OBC are efficient :

$$\bar{D}_t u = 0 \quad and \quad \bar{D}_t \omega = 0 \quad on\, \Gamma_{out} \quad (14)$$

where $\bar{D}_t = \partial_t + (\boldsymbol{U}.\nabla) = \partial_t + U\partial_x$ and where $\omega = \partial_x v - \partial_y u$ is the vorticity. Especially such OBC were found to be much more efficient than those simply involving the velocity components, both qualitatively and quantitatively. The vorticity isolines are very regular at the artificial outlet and an exponential-like decay of the error induced by the OBC is obtained in the upstream direction.

In the 3D case we suggest using:

$$\bar{D}_t u = 0 \quad and \quad \bar{D}_t(\boldsymbol{\omega} \times \boldsymbol{e}_x) = 0 \quad on\, \Gamma_{out} \quad (15)$$

which are coherent with the 2D case: it is the x-component of the velocity and the component of the vorticity vector in the $y-z$ plane (which reduces to ω_z in the 2D case) which are transported at the velocity U out of the computational domain. Note that as soon as $\bar{D}_t u = 0$,

$$\bar{D}_t \omega_z = \bar{D}_t(\partial_x v) \tag{16}$$
$$\bar{D}_t \omega_y = -\bar{D}_t(\partial_x w) \tag{17}$$

so that the OBC read:

$$\bar{D}_t u = 0, \quad \bar{D}_t(\partial_x v) = 0, \quad \bar{D}_t(\partial_x w) = 0 \quad on\, \Gamma_{out} \tag{18}$$

It is the consideration of a simplified problem, governed by the linearized incompressible Euler equations rather than the Navier-Stokes equations, which has yielded us to propose such OBC. Indeed, an homogeneous Neumann condition on the pressure is then only required at the outlet to yield a well-posed problem (see Appendix), but such a condition on the pressure is equivalent to $\bar{D}_t u = 0$. The other OBC are then nothing but the transport equations for the y and z-components of the vorticity, which simply results from taking the curl of the momentum equation. Notice that the consideration of the linearized Euler equations is also well justified, because no boundary layer occurs at Γ_h due to the free-slip boundary conditions.

Coming back to the stratified case, the temperature has simply to be transported at the mean velocity U and one has to take into account the buoyancy term when deriving the transport equation of the vorticity. Thus one obtains the following OBC:

$$\bar{D}_t T = 0 \tag{19}$$
$$\bar{D}_t u = 0 \tag{20}$$
$$\bar{D}_t(\partial_x v) = Ri \partial_x T \tag{21}$$
$$\bar{D}_t(\partial_x w) = 0 \tag{22}$$

To localize the effects of such OBC and so avoid upstream disturbances, our implementation of the $\bar{D}_t$ operator makes use of the method of characteristics. Thus, at the time-cycle $n+1$ one imposes at the outlet:

$$T^{n+1}(l) = T^n(l - U\tau) \tag{23}$$
$$u^{n+1}(l) = u^n(l - U\tau) \tag{24}$$
$$\partial_x v^{n+1}(l) = \partial_x v^n(l - U\tau) + \tau Ri \partial_x T^{n+1}(l) \tag{25}$$
$$\partial_x w^{n+1}(l) = \partial_x w^n(l - U\tau) \tag{26}$$

Moreover, an upwind quadratic interpolation procedure is simply used to compute the different variables at $x = l - U\tau$. Concerning the calculation of $\partial_x T^{n+1}$, we presently use

a first order finite-difference approximation, but one may remark that, from $\bar{D}_t T = 0$, one has also $\partial_x T = -\partial_t T/U$, which could be implemented consistently with the time-scheme.

Finally, let us mention that the following instability phenomenon has been observed: although using a divergence-free solver, the technique of characteristics does not yield OBC values which exactly respect the compatibility constraints resulting from the continuity equation (see [4]). The generalized Oseen problem is then ill-posed and the velocity field is no-more perfectly solenoidal. Such a phenomenon amplifies slowly in time, till inducing a divergence of the calculation. To overcome this difficulty, we use a least squares method to get an admissible outlet velocity profile from the advected one. This procedure is necessary to avoid the instability, although the difference between these two profiles is very small, say $O(10^{-8})$ in the max-norm.

4 MODELLING OF THE OBSTACLE

From the computational point of view, introducing an obstacle in a channel-like domain drastically transforms the standard cartesian domain in a complicated one. In the framework of high accurate methods, handling such geometries at a reasonable computational cost is not a trivial task. In order to retain the advantage of a simple computational domain, using a penalty technique, as e.g. in [5, 1], may be an alternative to spectral element or $h-p$ finite element methods, especially when the study of the details of the flow around the obstacle is not the main goal. Thus, for the study of far wakes it was interesting to consider the penalty technique and to check its capabilities in the framework of high order methods. Essentially we expect of such an approach a more realistic downstream flow than the one which would be obtained by prescribing a wake-type velocity profile.

In its basic formulation the penalty technique consists of introducing a body force term in the momentum equations, to vanish the velocity field $\boldsymbol{V}$ inside the obstacle. Thus, the momentum equation is rewritten as :

$$\begin{aligned} \partial_t \boldsymbol{V} + (\boldsymbol{V}.\nabla)\boldsymbol{V} &= -\nabla p + \frac{1}{Re}\Delta \boldsymbol{V} + C f(\boldsymbol{x})\boldsymbol{V} \\ \nabla \cdot \boldsymbol{V} &= 0 \end{aligned}$$

In this equation the coefficient C should be chosen as $C = \infty$ and $f(\boldsymbol{x})$ as the characteristic function of the obstacle. However, in practice the constant C is adjusted to approximatively vanish the velocity inside the obstacle and, to avoid the Gibbs phenomenon, the characteristic function is filtered. Thus, we generally choose $C \approx 10^2$ and the raised cosine filter (see e.g [3]) to obtain $f(\boldsymbol{x})$.

To check the capabilities of this approach the 2D and 3D wakes behind a cylinder have been computed and our results have been compared to those of different authors. No stratification was considered in these preliminary tests.

First, the 2D case was considered with a Reynolds number $Re = 200$, corresponding to the 2D-3D transition. As usual, the characteristic length and velocity equal the cylinder

diameter and the fluid inflow velocity respectively. For such a value of Re the flow is unsteady and a von Karman street develops behind the cylinder. Calculations were made in the domain $\Omega =]0, 20[\times]-4, 4[$, using for the space approximation $N = 5, I = 50, J = 100$ and the time-step $\tau = 5.10^{-3}$. Fig. 1 shows the vorticity field obtained at time $t = 190$. As could be expected the constant C value is a little low, so that the cylinder is only described approximatively. Nevertheless, the Strouhal number equals $St \approx 0.19$, in satisfactory agreement with the values obtained in the calculations of [2] ($St \approx 0.20$), [9] ($St \approx 0.21$) or [10] ($St \approx 0.19$), where a similar penalty method is used.

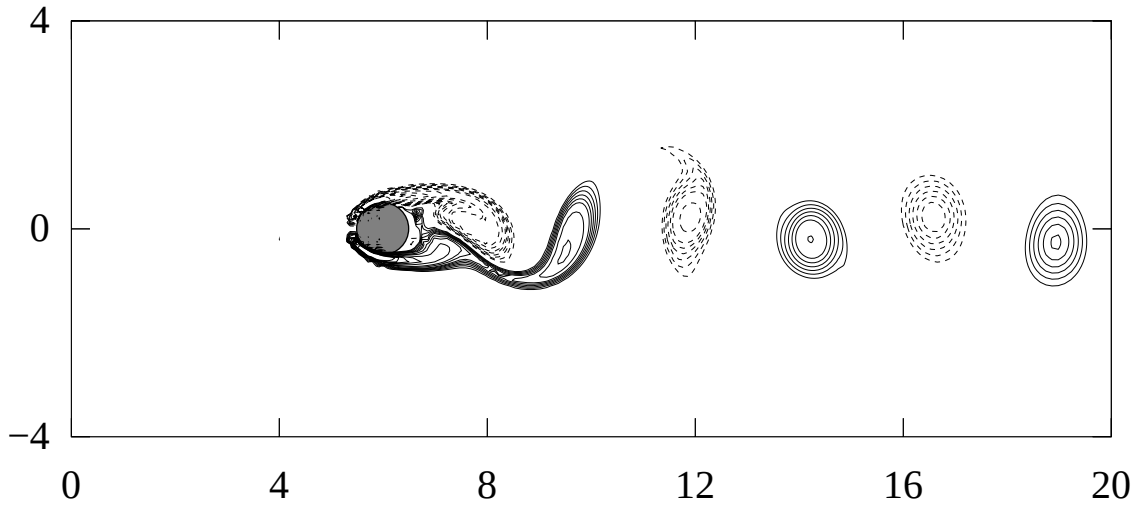

Figure 1: Vorticity at time $t = 190$, $Re = 200$.

When using the penalty technique the determination of the drag and lift coefficients resume to an integration of the force field in any cartesian domain in which the obstacle is embedded (at least in the limit $C = \infty$ and without filtering of $\boldsymbol{f}(\boldsymbol{x})$). Here it is convenient to choose as integration domain the computational subdomain, say Ω_l, surrounding the cylinder. Accurate integrations can then be carried out using the Gauss-Lobatto quadrature formula, slightly modified to support non-linear coordinate transforms. The dimensionless resultant $\boldsymbol{F}$ of the force field reads :

$$\boldsymbol{F} = \int_{\Omega_l} C f(\boldsymbol{x}) \boldsymbol{V} d\Omega = \int_{\Omega_l} \partial_t \boldsymbol{V} \, d\Omega + \int_{\partial\Omega_l} [\boldsymbol{V}\boldsymbol{V} + p\mathbf{1} - \frac{1}{Re}(\nabla \boldsymbol{V} + (\nabla \boldsymbol{V})^t)].\boldsymbol{n} \, d\Gamma \qquad (27)$$

where $\boldsymbol{n}$ is the unit outwards vector normal to $\partial\Omega_l$. Of course, such an expression simplifies when taking into account the free-slip boundary condition on Γ_h. In Fig. 2 we show the time-variations of the drag and lift coefficients, equal to $C_x = -2\,F_x$ and $C_y = -2\,F_y$ respectively. Such results, which again point out the value of the Strouhal number, compare rather well for example with those given in [10].

Second, the 3D flow was computed for two different values of the Reynolds number: $Re = 220$ and $Re = 300$. These values are especially interesting because they correspond

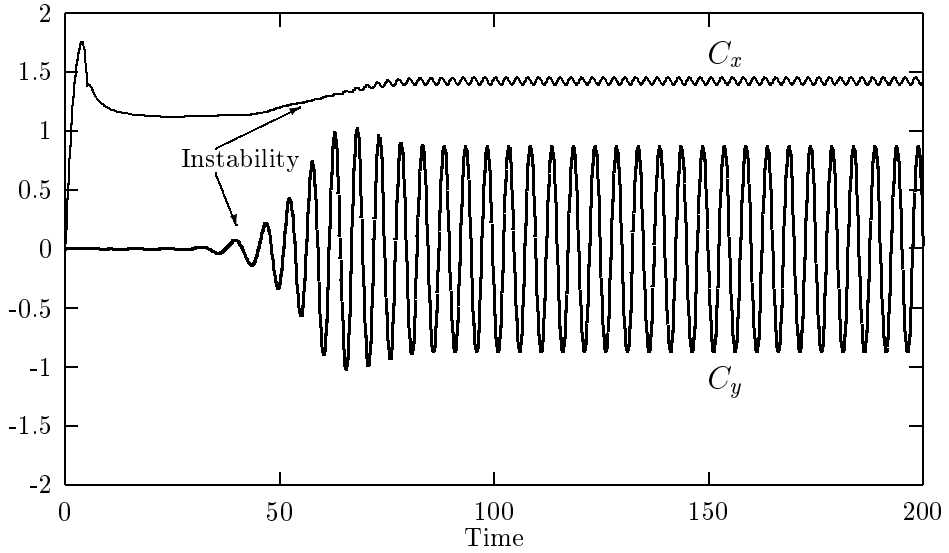

Figure 2: Lift and drag coefficients vs time.

to two different 2D-3D transitions [14]. For $Re = 220$, one gets the so-called "mode A" instability, essentially characterized by a periodicity of the wake vortical structure equal to four diameters, whereas for $Re = 300$ one gets the "mode B", for which the periodicity equals one diameter. Moreover, in the streamwise direction the iso-vorticity structures are of the same sign for the mode A, whereas one observes alternative signs for the mode B. In Fig. 3 are presented iso-surfaces of the x and y-components of the vorticity vector, which point out the 3D feature of the flow. Such results compare well with the visualizations presented in [15]. The calculations have been carried out with $N = 5$ subdomains, $I = 40$, $J = 81$, $K = 24$ and a time-step $\tau = 10^{-2}$ in the domain $\Omega =]0, 20[\times] - 4, 4[\times 0, 4[$. Thus, although remarks may be expressed, (i) concerning the real value of the cylinder diameter and consequently of the effective Reynolds number value and (ii) the fact that the velocity does not exactly vanish inside the cylinder ($|\boldsymbol{V}| \approx 10^{-2}$), one observes here that the penalty technique has permitted to recover results not easy to capture numerically.

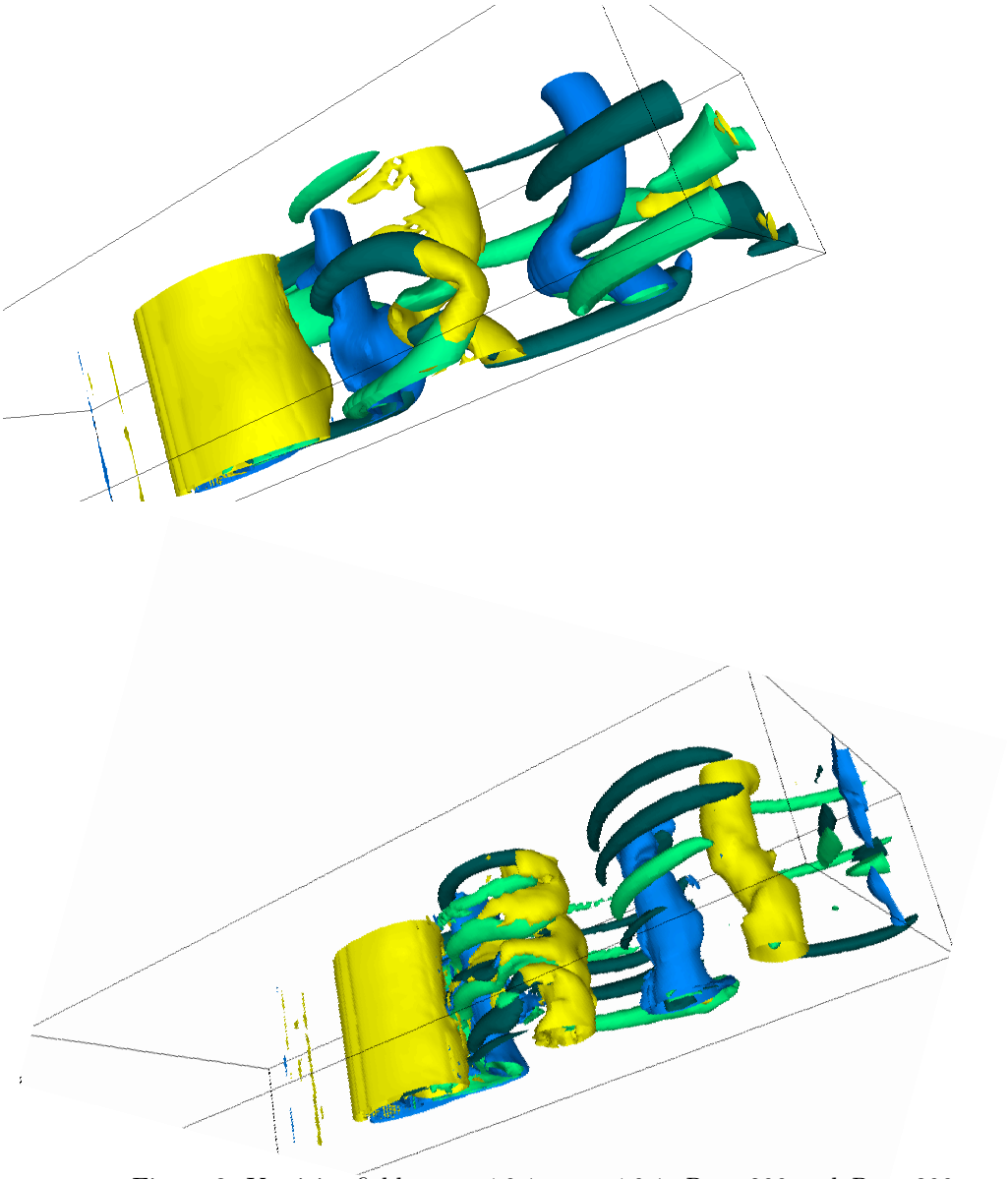

Figure 3: Vorticity field, $\omega_x = \pm 0.1, \omega_z = \pm 0.1$, $Re = 200$ and $Re = 300$.

5 WAKES OF A SPHERE IN STRATIFIED FLUIDS

Here we present results obtained for the wake behind a sphere in fluids stably stratified by a constant thermal gradient. For the characteristic parameters we use $Pr = 7$, $Re = 300$ and three values of the Richardson number, $Ri = \{0, 0.04, 0.25\}$. In case $Ri = 0$, the temperature evolves as a passive scalar. Notice that results at a lower Reynolds number, $Re = 200$, are presented in [7] and that the case of strong stratification is investigated in [5].

The main difficulties of the numerical study are due to the high value of the Peclet number, $Pe = Pr\,Re = 2100$. Especially, to improve the stability of the time-scheme, we use sub-time cycling to solve the temperature equation (3 sub-time-steps). More subtle is the difficulty coming from using a multi-domain technique, which induces, when the diffusion term is negligible, the presence of pseudo-spurious modes for the temperature. They manifest by (i) slight oscillations of $T(x, y, z)$ in x-direction and by (ii) small jumps at the interfaces of the sub-domains. This pseudo-spurious mode problem results from the fact that Dirichlet conditions are imposed at the interfaces, in the framework of our multi-domain technique, so that the Chebyshev polynomial $T_I(x) = \cos(I \cos^{-1} x)$ tends to become spurious when the diffusive term tends to vanish. In order to overcome this difficulty filtering is used in the x-direction, i.e. the higher Chebyshev mode in x is set equal to 0.

The computational domain is $\Omega =]0, 29[\times]-3, 3[\times]0, 6[$ and the sphere is centered at $(8.5, 0, 3)$. For the space approximation we use $N = 17$ subdomains of different width and $I = 30, J = 72, K = 36$, in each of them. The center of the sphere is located at the interface of two subdomains, of width 1, and coordinate transforms are implemented both in the x and y directions to get a good approximation of the sphere with the penalty technique. The time step equals $\tau = 5.10^{-3}$.

The characteristic length is the diameter of the sphere, the characteristic velocity is the inlet one and the characteristic temperature equals its vertical variation with respect to the characteristic length, so that at the initial time $T = y$. This linear variation of the temperature is used as Dirichlet condition at the inlet.

First a calculation has been carried out with $Re = 100$ and $Ri = 0$, till obtaining a quasi-axisymmetric steady flow. This steady flow has then been used as initial condition, say at $t = 0$, to compute the flow with $Re = 300$ and $Ri = 0$, i.e. without influence of the temperature on the flow, till the time $t = 60$. Moreover, in order to induce an instability, a random perturbation of the velocity field has been used at time $t = 5$. The instability manifests later, at $t \approx 30$. As expected from experimental observations [11] and from calculations [8], the flow is symmetric with respect to the plane $y = 0$. This symmetry plane is not arbitrary, but clearly associated with the boundary conditions used for the velocity in the planes $y = \pm 3$ (free-slip) and $z = \{0, 6\}$ (periodicity).

Calculations have been continued till time $t = 120$, with $Re = 300$ and for the different values of the Richardson number: $Ri = \{0, 0.04, 0.25\}$. Let us emphasize that these values correspond to the case of weak stratification: in terms of the internal Froude number (based on the diameter of the sphere), $Fi = Ri^{-1/2}$, one obtains $Fi = \infty$, $Fi = 5$ and $Fi = 2$, so that with $Re = 300$ we do not expect the quasi-two-dimensional flows obtained in case of strong stratification [12]. On the contrary, we investigate the transitional range inside which the stratification becomes active.

For the three values of the Richardson number and at the final time $t = 120$, Fig. 5 to 10 show opposite iso-surfaces of the x-component of the vorticity and opposite iso-surfaces of the temperature. As may be observed, the influence of the stratification

manifests clearly, especially for the highest value of the Richardson number, and the flow is no-longer perfectly symmetric with respect to the plane $y = 0$.

In order to get more details on the vorticity and temperature fields, isolines in cross-sections at different values of x and at $t = 120$ are also presented. The oscillating motion in the horizontal plane is essentially induced by pairs of vortices of opposite signs, at the interface of which a new pair of vortices forms, amplifies before inducing an horizontal motion of opposite sense. This is especially visible with $Ri = 0$. For the non null values of Ri the phenomenon is similar, but the buoyancy forces tend to maintain pairs of vortices at the end-sides of the wake. The isotherms also point out the horizontal motion as well as the influence of the stratification. However, on the contrary of the vorticity field, whose intensity is decreasing with x, the distortion of the temperature field is increasing.

Finally let us mention that such flows are not yet periodic and so that the Strouhal number cannot be estimated accurately, as shown by the Fig. 4 which gives the evolution of the u-component of the velocity at point $(16, 0, 3.5)$ for the three different values of Ri. However, it is interesting to note that the periodic behaviour is better established for $Ri = 0.25$, for which we can get the crude estimate $St \approx 0.09$, and that an increase of Ri seeems to induce a decrease of the Strouhal number. Let us recall that in case $Ri = 0$, the experiments give $St \approx 0.15$ and the calculations of [8] $St \approx 0.135$.

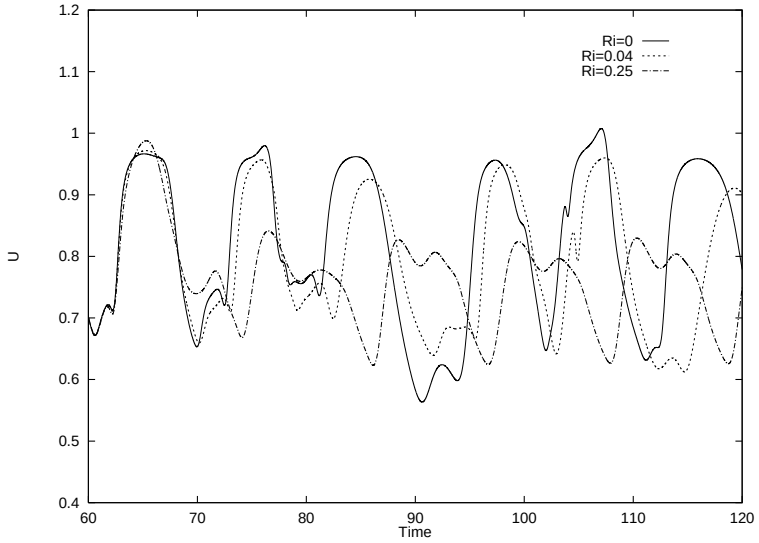

Figure 4: u, for $Ri = \{0, 0.04, 0.25\}$, vs time.

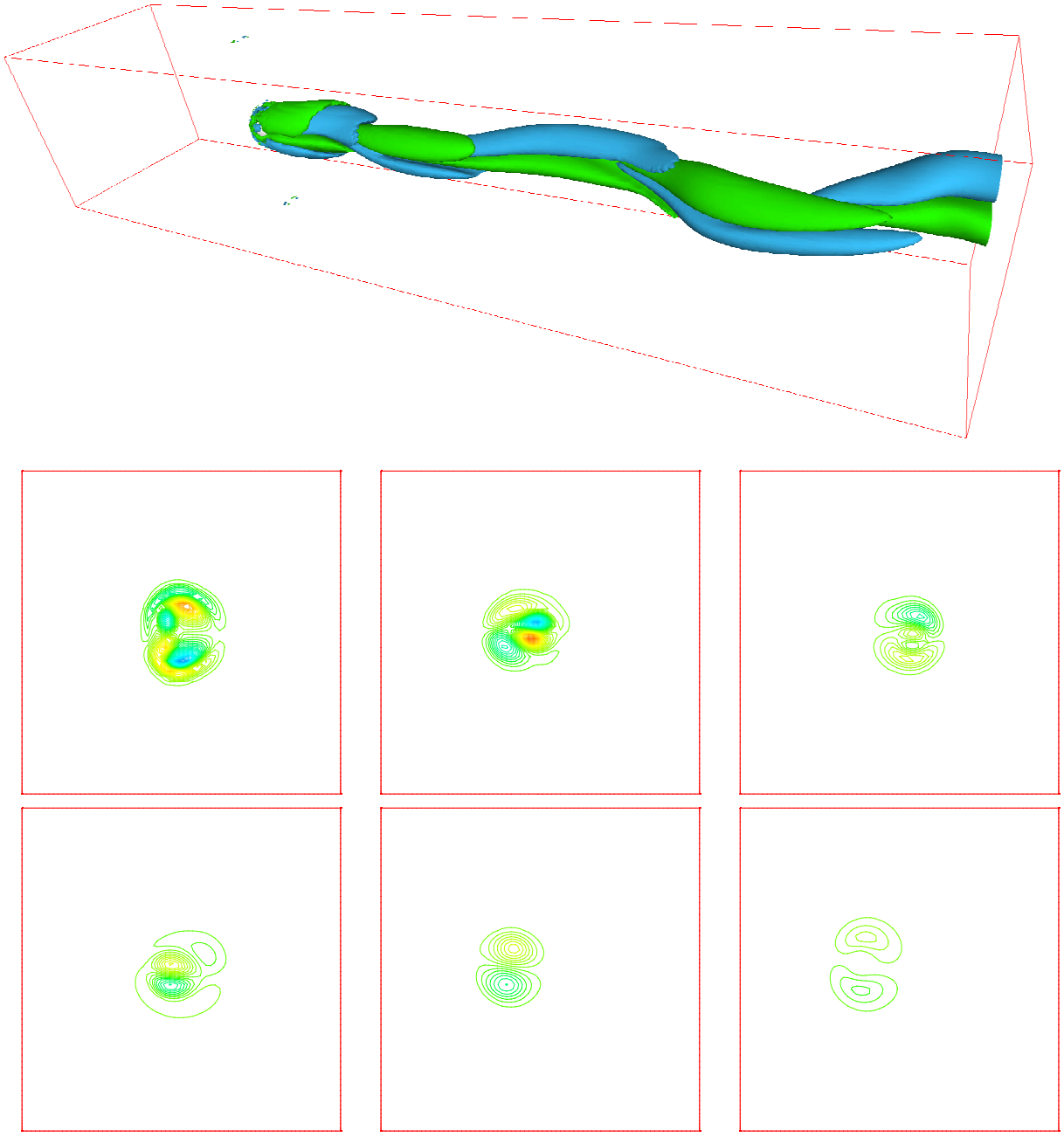

Figure 5: Vorticity field (x-component), $Re = 300$, $Ri = 0$, above: isosurfaces $\omega_x = \pm 0.1$, below: isolines in cross-sections $x = \{10, 12, 14, 16, 18, 20\}$, $-2.9 \leq \omega_x \leq 2.9$.

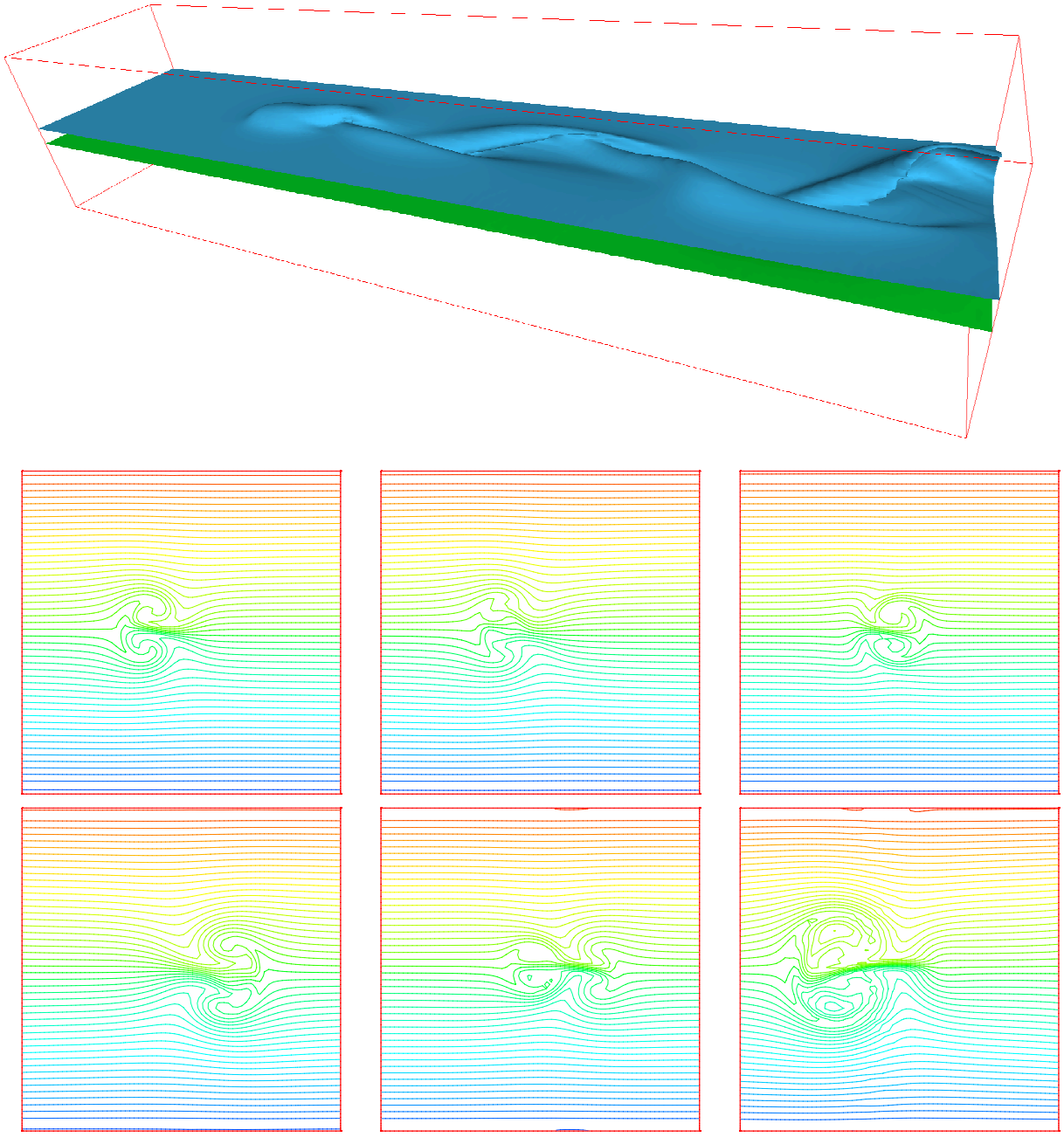

Figure 6: Temperature field, $Re = 300$, $Ri = 0$, above: isosurfaces $T = \pm 0.3$, below: isolines in cross-sections $x = \{18, 20, 22, 24, 26, 28\}$.

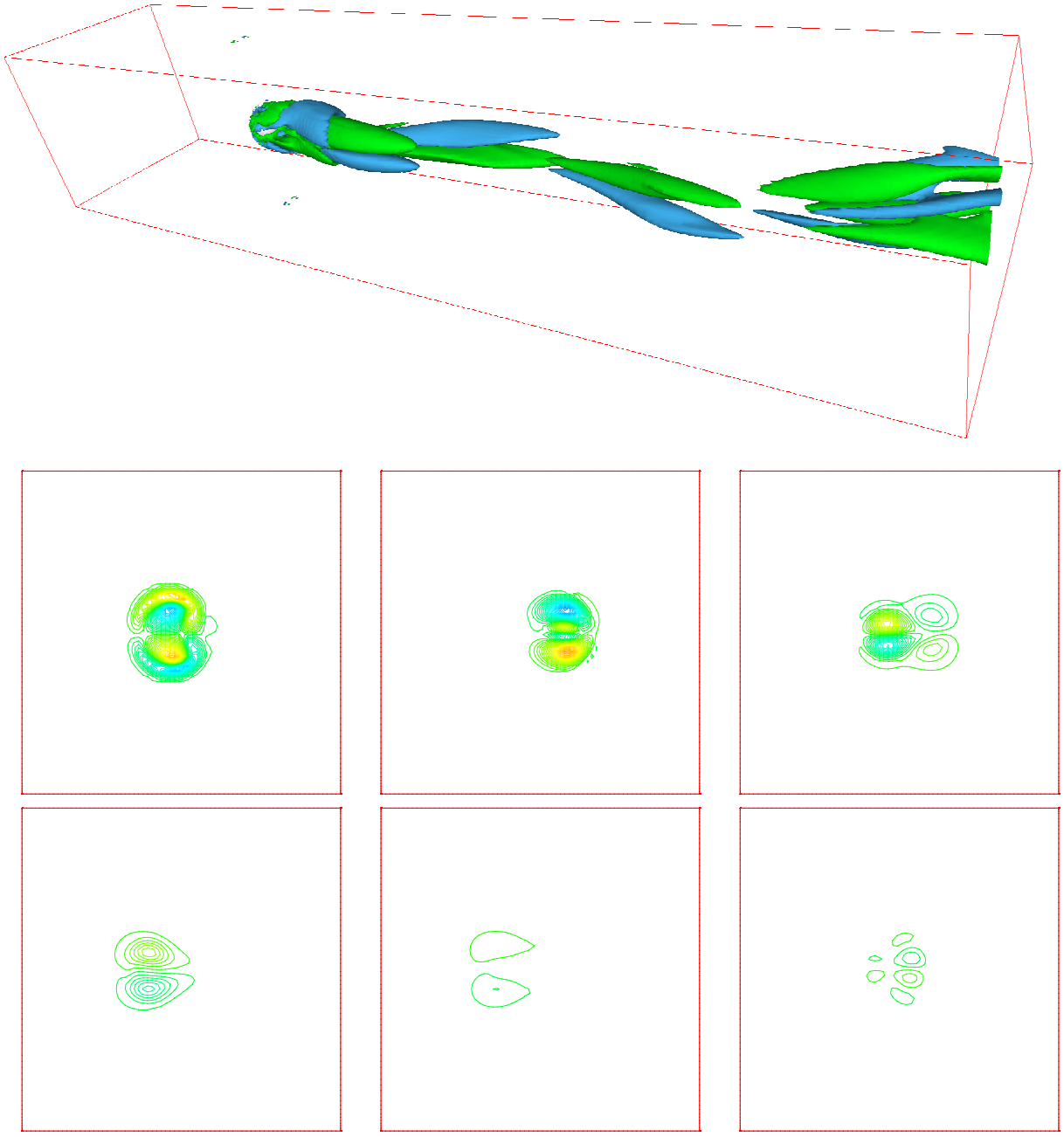

Figure 7: Vorticity field (x-component), $Re = 300$, $Ri = 0.04$, above: isosurfaces $\omega_x = \pm 0.1$, below: isolines in cross-sections $x = \{10, 12, 14, 16, 18, 20\}$, $-2.9 \leq \omega_x \leq 2.9$.

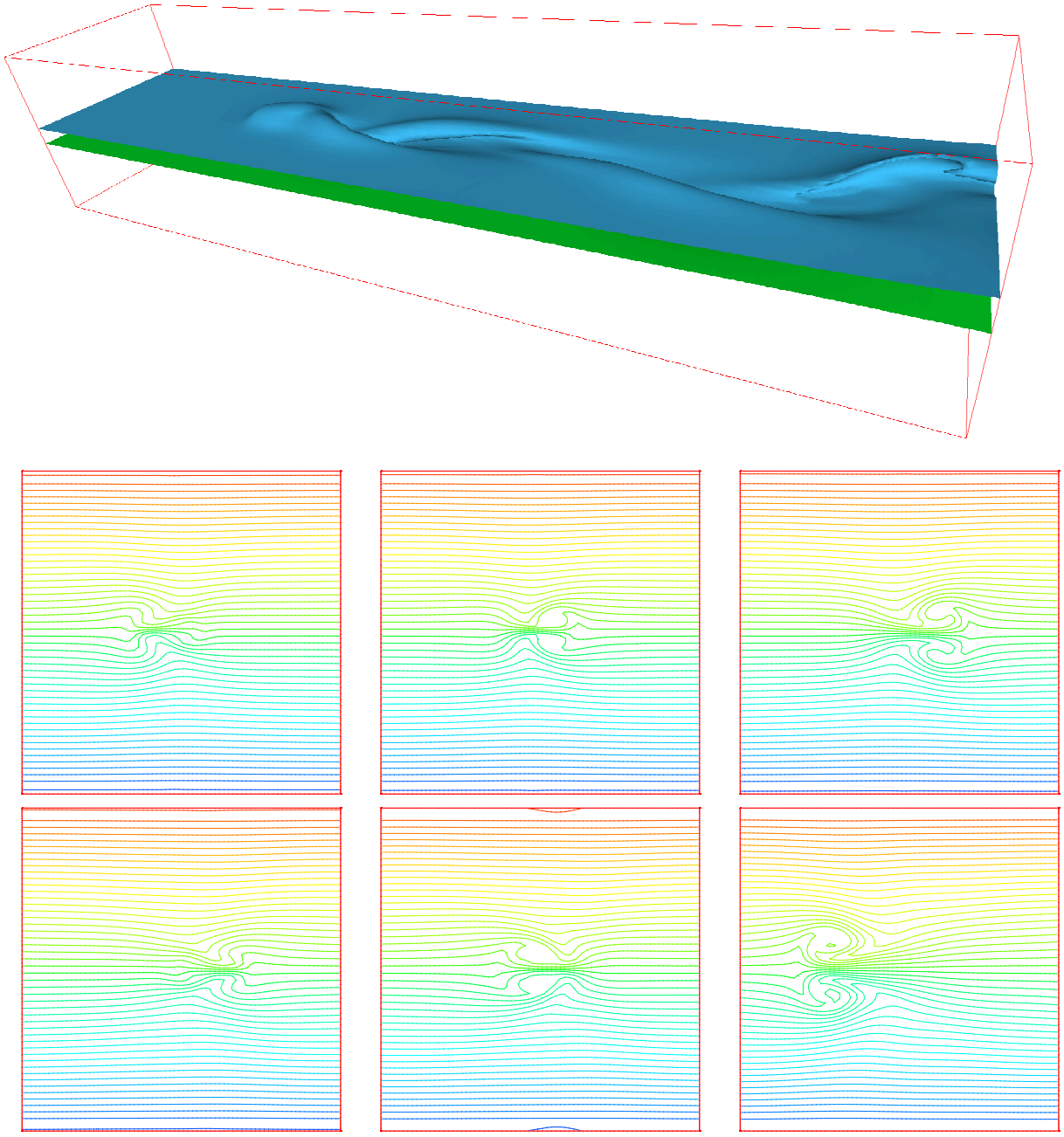

Figure 8: Temperature field, $Re = 300$, $Ri = 0.04$, above: isosurfaces $T = \pm 0.3$, below: isolines in cross-sections $x = \{18, 20, 22, 24, 26, 28\}$, $-3 \leq T \leq 3$.

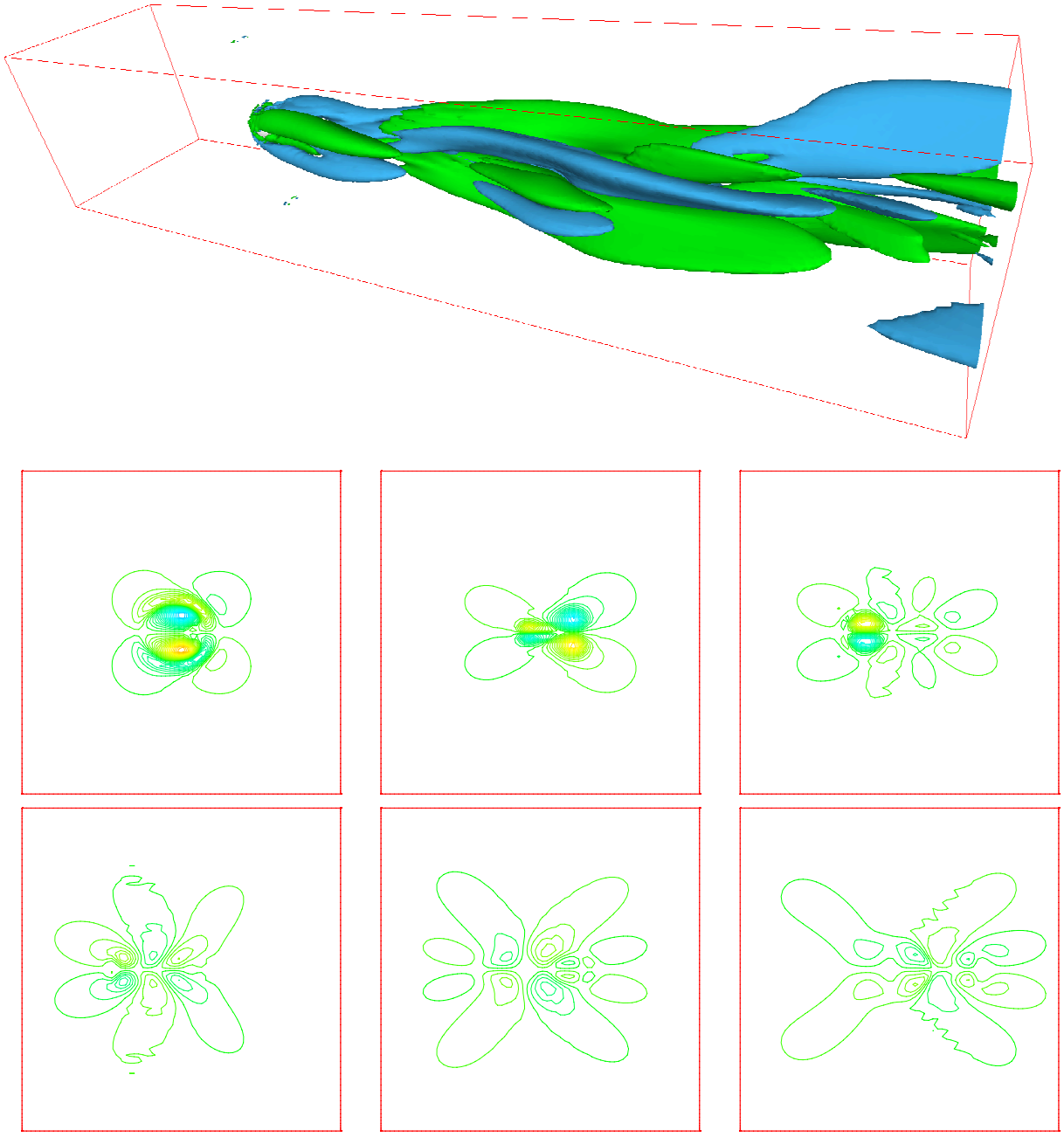

Figure 9: Vorticity field (x-component), $Re = 300$, $Ri = 0.25$, above: isosurfaces $\omega_x = \pm 0.1$, below: isolines in cross-sections $x = \{10, 12, 14, 16, 18, 20\}$, $-2.9 \leq \omega_x \leq 2.9$.

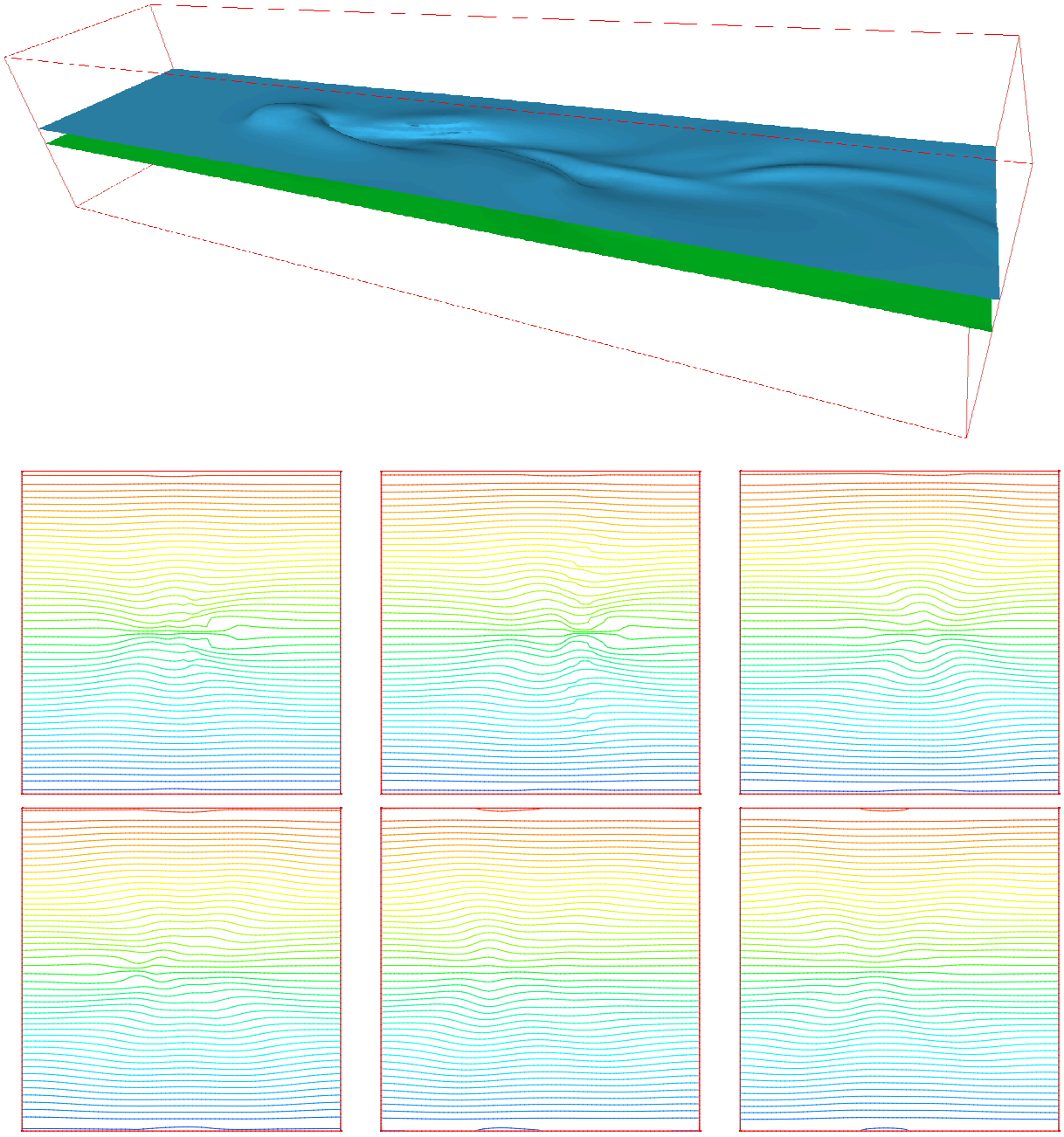

Figure 10: Temperature field, $Re = 300$, $Ri = 0.25$, above: isosurfaces $T = \pm 0.3$, below: isolines in cross-sections $x = \{18, 20, 22, 24, 26, 28\}$, $-3 \leq T \leq 3$.

6 CONCLUSION

A highly accurate numerical method has been developed for the computation of far wakes in stratified fluids. In this paper we have especially focused on some sensitive points, like the outflow boundary conditions or the penalty technique to model the obstacle. Considering the case of a sphere immersed in water, our first investigations, at $Re = 300$, of the weak stratification case, $Ri = \{0, 0.04, 0.25\}$, have permitted to recover results recently obtained without stratification and to point out the influence the buoyancy forces on the spatial development of the wake.

Acknowledgments This study was supported by the CNRS and the "région PACA". The calculations have been performed on the CRAY T3E supercomputer of the IDRIS french center. We are grateful to J.M. Lacroix for his technical support.

APPENDIX

To justify the OBC proposed in section 3, we consider the linearized Euler equations and show that an homogeneous Neumann boundary condition on the pressure, at the outlet, yields a well-posed problem. For each Fourier mode number k the problem reads:

$$\begin{aligned}
\bar{D}_t \hat{\boldsymbol{v}}_k &= -\nabla_k \hat{p}_k && (28)\\
\nabla_k . \hat{\boldsymbol{v}}_k &= 0 && (29)\\
\hat{\boldsymbol{v}}_k . \boldsymbol{e}_y &= 0 \quad at \quad \Gamma_h && (30)\\
\hat{\boldsymbol{v}}_k &= \hat{\boldsymbol{v}}_{kin} \quad at \quad \Gamma_{in} && (31)\\
\partial_x \hat{p}_k &= 0 \quad at \quad \Gamma_{out} && (32)\\
\hat{\boldsymbol{v}}_k(t=0) &= \hat{\boldsymbol{v}}_{k0} && (33)
\end{aligned}$$

where $\nabla_k = (\partial_x, \partial_y, \mathrm{i}k)$, with $\mathrm{i}^2 = -1$. Of course, $\hat{\boldsymbol{v}}_{kin}$ is supposed to be time and space dependent.

Assuming the velocity and pressure fields sufficiently regular, from the divergence of the momentum equation, the boundary conditions on the velocity $\hat{\boldsymbol{v}}_k = (\hat{u}_k, \hat{v}_k, \hat{w}_k)$ and the continuity equation, one obtains for $\hat{p}_k$:

$$\begin{aligned}
\nabla_k^2 \hat{p}_k &= 0 && (34)\\
\partial_y \hat{p}_k &= 0 \quad at \quad \Gamma_h && (35)\\
\partial_x \hat{p}_k &= -\partial_t \hat{u}_k + U(\partial_y \hat{v}_k + \mathrm{i}k\hat{w}_k) \quad at \quad \Gamma_{in} && (36)\\
\partial_x \hat{p}_k &= 0 \quad at \quad \Gamma_{out} && (37)
\end{aligned}$$

If $k \neq 0$, this problem is well-posed and yields $\hat{p}_k$. If $k = 0$, then $\hat{p}_k$ may be determined up to a constant as soon as the compatibilty condition :

$$\int_{\Gamma_{in}} (-\partial_t \hat{u}_k + U \partial_y \hat{v}_k)\, d\Gamma = 0 \qquad (38)$$

is satisfied. This directly results from the null value of $\hat{v}_k$ at Γ_h and from the definition of $\boldsymbol{v}$ as the deviation of the mean velocity.

Consequently, $\hat{\boldsymbol{v}}_k$ simply solves the 1D advection problem (28), y being a parameter, whose solution only requires the initial condition (33) and the boundary condition (31) at the inlet.

REFERENCES

References

[1] P. Angot, C.H. Bruneau and P. Fabrie, A penalization method to take into account obstacles in incompressible viscous flows, *J. Numer. Math.*, **81**, pp. 497-520 (1998).

[2] M. Braza, P. Chassaing and H. Ha Minh, Numerical study and physical analysis of the pressure and velocity fields in the near wake of a circular cylinder, *J. Fluid Mech.*, **165**, pp. 79-130 (1986).

[3] C. Canuto, M.Y. Hussaini, A. Quarteroni and T.A. Zang, *Spectral Methods in Fluid Dynamics*, Springer, Berlin (1988).

[4] M.Y. Forestier, R. Pasquetti, R. Peyret and C. Sabbah, Spatial development of wakes using a spectral multi-domain method, *ICOSAHOM'98 Congress*, to be published in *Appl. Num. Math.*.

[5] Y.T. Fung and S.W. Chang, Surface and internal signatures of organized vortex motions, *Phys. Fluids*, **8**, pp. 3023-3056 (1996).

[6] S.V. Tsynkov, Numerical solutions of problems on unbounded domains, *Appl. Num. Math.*, **27**, pp. 465-532 (1998).

[7] H. Hanazaki, A numerical study of three-dimensional stratified flow past a sphere, *J. Fluid Mech.*, **192**, pp. 393-419 (1988).

[8] T.A. Johnson and V.C. Patel, Flow past a sphere up to a Reynolds number of 300, *J. Fluid Mech.*, **378**, pp. 19-70 (1996).

[9] G.EM Karnadiakis and G.S. Triantafyllou, Frequency selection and asymptotic states in laminar wakes, *J. Fluid Mech.*, **199**, pp. 441-469 (1989).

[10] K. Khadra, P. Angot, S. Parneix and J.P. Caltagirone, Fictitious domain approach for numerical modelling of Navier-Stokes equations, *Int. J. Numer. Methods Fluids*, to be published.

[11] T. Leweke, M. Provansal, D. Ormières and R. Lebescond, Vortex dynamics in the wake of a sphere, *Phys. Fluids*, **11**, pp. 3023-3056 (1999).

[12] Q. Lin, W.R. Lindberg, D.L. Boyer and H.J.S. Fernando, Stratified flow past a sphere, *J. Fluid Mech.*, **240**, pp. 315-354 (1992).

[13] C. Sabbah and R. Pasquetti, A divergence-free multi-domain spectral solver of the Navier-Stokes equations in geometries of high aspect ratio, *J. Comput. Phys*, **139**, pp. 359-379 (1998).

[14] C. H. K. Williamson, Vortex dynamics in the cylinder wake, *Annu. Rev. Fluid. Mech.*, **28**, pp. 477-539 (1996).

[15] H. Zhang, U. Fey, B.R. Noack, M. König, H. Eckelmann, On the transition of the cylinder wake, *Phys. Fluids*, **7**, pp. 779-794 (1995).